Colloid Polym Sci 278:964–971 (2000)

ORIGINAL CONTRIBUTION

V. Pedroni
P. C. Schulz
M. E. Gschaider de Ferreira
M. A. Morini

A chitosan-templated monolithic siliceous mesoporous-macroporous material

Received: 12 January 2000
Accepted: 7 March 2000

V. Pedroni · P. C. Schulz (✉)
M. E. Gschaider de Ferreira
M. A. Morini
Departamento de Química e Ingeniería Química, Universidad Nacional del Sur
8000 Bahía Blanca, Argentina
e-mail: pschulz@criba.edu.ar

Abstract We synthesised a porous siliceous material via hydrothermal hydrolysis of sodium silicate, using chitosan as a template. As far as we know, this is the first synthesis of siliceous porous material using chitosan as a template in a hydrothermal way. A fibrous material was obtained, whose macroscopic fibres were formed by a spongelike siliceous network with pores having a radius of 0.57 μm. The siliceous walls of the pores were, in turn, of the form of a microporous–mesoporous material; the pore radius distribution was polymodal with maxima at 0.84, 1.0, 1.2 and 1.5 nm and a broad band between 3 and 10 nm. This structure may be due to the aggregation of the hydrated chitosan helices in bundles of parallel fibres with different size and the gelation of the system. The aggregation process might be induced by the addition of silicate.

Key words MCM-41 synthesis · Chitosan · Mesoporous–macroporous material · Monolithic material

Introduction

Porous materials containing interconnected microscopic and macroscopic cavities, for example, sponges, clays, ceramics and different polymeric systems, are of outstanding importance in industry and everyday life. The spectrum of applications consists of all types of filtration, extraction, adsorption, catalyst carriers, drug delivery systems, environmental remediation materials [1] and shape-selective reactors for polymerisation [2], membrane separators and stationary phases for chromatography [3].

In view of the extensive possibilities for the application of these materials, the obtaining of novel structures and novel synthesis procedures is of great interest.

In 1992, Mobil's scientists discovered that ionic surfactants could be used as templates for the synthesis of a family of mesoporous siliceous materials which they called M41S [4, 5].

One of the most studied of these structures is the MCM-41 material, with unidirectional mesopores ordered in a hexagonal array and a sharp pore size distribution, which is obtained using cationic surfactants in dilute (micellar) or liquid-crystalline conditions. To modify the pore size, higher homologues of the surfactant series and inert oils as swelling agents are used.

The template strategy resembles macroscopic metal casting processes: geometrically well defined structures (''templates''), which perform the shapes of the pores like casting cores, are introduced into a liquid system and subsequently embedded by hardening of the solvent. After removal of these cores from the surrounding matrix the shape of the remaining voids reflects the form of the templates.

Ultra-large-pore hexagonal and cubic mesoporous products have recently been synthesised using nonionic poly(ethylene oxide) triblock copolymers as structure-directing agents [6–8]. Recently a fibrous bacterium, *Bacillus subtilis*, was the substrate used for the deposition of an MCM-41-type material [9], leading to materials with porosity in both the mesoscopic (2–10 nm) and macroscopic (0.5 μm) ranges after the bacteria were removed from the composite material by calcination.

Macromolecular templates have been used to produce organic mesoporous materials by polymerisation of aqueous acrylamide solutions in the presence of xanthan or DNA fragments. Hydrogels containing nonoriented channels with diameters from 2 to 10 nm have been obtained [10]. Some cationic and anionic block copolymers with polyelectrolyte behaviour were also utilised as structure-directing media in a sol–gel process to synthesise nanoporous silica [8].

The previously mentioned considerations led us to suppose that some natural polymers might be used as templates in the production of porous materials. In particular, we thought about the cationic polyelectrolyte chitosan, which may be used in conditions similar to that of cationic surfactants. The physicochemical properties of chitosan seemed to be a source of different structures in solution, which might provide novel porous materials.

Chitosan, a (1-4)-linked 2-amino-2-deoxy-β-D-glucopiranose, is a polymer derived from chitin. Chitin is typically extracted from the shells of crustaceans such as shrimp, crab, lobster and squid. This natural polymer may also be found in the shells of some insects, such as beetles, and in some fungi. It is the second most abundant natural polymer after cellulose [11]. Chitosan is the *N*-deacetylated form of chitin. Chitosan is well known as a nontoxic and biodegradable linear polymer. It is widely used in the medical industry in products ranging from burn dressings to drug delivery capsules. The term chitosan is usually reserved for chitin molecules that are deacetylated to the point where they become soluble in dilute aqueous acidic systems (e.g., 1–10% by volume acetic acid). The percentage of deacetylation is usually named the deacetylation degree (DD). Chitosan becomes soluble in aqueous acidic solutions when DD exceeds 50%. DD = 100% is very difficult to achieve. A molecular illustration of chitosan can be found in Fig. 1. The amino and acetamide groups are randomly distributed along the backbone of all acid-soluble chitosans, following Bernoullian distributions [12–14].

The crystalline structure of chitosan has been described as an extended twofold helix stabilised by intramolecular hydrogen bonds [15–18]. Three forms of solid chitosan have been found: hydrated [19], anhydrous crystals [20] and noncrystal line. A chitosan sample rich in anhydrous crystals cannot be dissolved

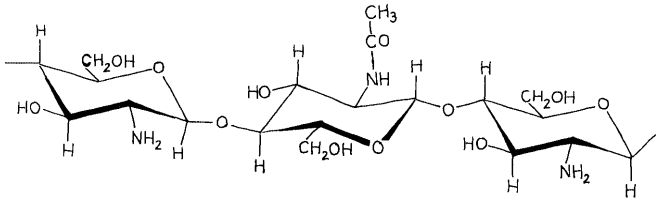

Fig. 1 A schematic illustration of the structure of chitosan

with any chitosan solvents, such as acetic acid. The structure of anhydrous chitosan crystals was found to be monoclinic, the unit cell having $a = 1.38$ nm, $b = 1.63$ nm, $c = 4.07$ nm (parallel to the molecular axis), $\alpha = 96.46°$ [16]. The hydration of chitosan produced an orthorhombic unit cell ($a = 0.89$, $b = 1.70$ nm, $c = 1.025$ nm) [19]. Some chitosan salts crystallise in a monoclinic unit cell with a helical repetition of 4.073 nm, with the backbone adopting a helix conformation [21].

Due to the presence of protonated amino groups (the amino group in chitosan has a pK_a of about 6.2–7 [22, 23]), chitosan in dilute acid aqueous solution exhibits polyelectrolyte character at low pH (below pH 6.5) and its hydrodynamic behaviour in the solution is intricate [24–28]. Polycations are rare in nature and chitosan is the only case in the family of polysaccharides. The repulsion of the positive charges on the amide groups along the backbone chain will certainly make a stretched chain in solution. Besides the polyelectrolyte effect, the *n*-acetyl groups also influence the chain conformation [27]. The solubility is also favoured by the hydration of various sites, mainly those which are charged.

The intramolecular hydrogen bonds are probably maintained in solution. Wu et al. [29] stated that the chitosan chain is slightly extended in aqueous solution and that even in dilute solution chitosan still forms a small number of large-sized aggregates. In dilute solutions, chitosan molecules follow the structure of wormlike chains [30]. The chain conformation in solution is strongly influenced by ionic strength and DD. The lower the ionic strength, the more extended the molecule [31].

Chitosan exhibits interesting association and gelling properties [32–38] in aqueous solution under various conditions. Supramolecular structures, which have hydrogen-bonding, van der Waals and hydrophobic interactions among neighbouring units were revealed by electron microscopy [31]. It has been shown that the dissolution of the chitosan molecules was conditioned by the memory of the crystalline arrangement in the solid state with preservation of some supramolecular organisations [39].

Wu et al. [29] found that even in dilute solution chitosan still forms a small number of larger sized aggregates. At higher concentration, chitosan, mainly those samples with higher molecular weight, forms larger aggregates [33, 40] and a gel [41]. This behaviour must be related to the formation of local hydrophobic contacts, or hydrogen bonding, responsible for a more or less important physical reticulation of chitosan chains [42]. It has also been shown that the chitosan/water system exhibits liquid-crystalline mesophases for a water-weight concentration higher than 44% [43]. It seems that the addition of low-molecular-weight electrolytes is not able to completely eliminate the

polyelectrolyte effect and hydrogen bonding between different chitosan chains, but nevertheless promotes aggregation.

Other related associative gelling systems (polysaccharides) undergo a disorder-to-order molecular conformational transition (e.g., coil to helix or multiple helix) induced either thermally or by the addition of salts. This is usually the significant step. Gel character then results either through weak association (and/or entanglement) of the stiffened structures (weak gel formation) or through stronger interactions. The latter includes cross-linking of multiple helices through imperfect matching of chains and interactions involving substantial lateral helix association (strong gels). Networks of all these types are exemplified by the bacterial polysaccharide xanthan gum (weak gel network) and by the marine algae polysaccharides ι-carrageenan (little helix association) and agarose (substantial helix association) [44]. The existence of helix conformations and multiplicity in polysaccharide solutions was demonstrated in a number of works. For example, light scattering [45] and neutron scattering studies [46, 47] of xanthan solutions support a double-stranded helix for this molecule when it is ordered under appropriate conditions of temperature, polymer concentration and ionic strength; the double helical structures proposed to underlay carrageenan gels and gels from agarose have received confirmation from light scattering studies [48]. The κ-carrageenan sol was described as containing a wormlike polyelectrolyte in semidilute conditions, whilst the gel was based on bundles of parallel double helices [49].

On the basis of this information, we assumed that the helical structures of chitosan in solution could serve as templates for the production of mesoporous silica materials. The pore diameter would probably be that of the hydrated helix, in the case of isolated molecules, or that of the aggregates. If gelling were induced by the addition of sodium silicate, the structure of the gel would serve as a template. In both cases, novel porous material would be obtained. We used a very dilute solution of chitosan in order to avoid the formation of large aggregates.

We also synthesised an MCM-41 sample for comparison.

Experimental

Chitosan (Daras) of molecular weight 223 872 with 11% water content and 0.38 ash, DDA = 84%, viscosity 50 mPa s was used without further purification.

MCM-41 synthesis

Pure siliceous MCM-41 was prepared by addition of 6.2 g sodium silicate to a solution of 0.2 ml H_2SO_4 (Carlo Erba, 96%) in 13.3 ml double-distilled water. After stirring for 10 min, a solution of 5.59 g of cetyltrimethylammonium bromide (CTAB) in 16.75 ml water was added, followed by 30 min of stirring. Then, 6.6 ml water was added and the gel was stirred for 30 min. The mixture was autoclaved at 140 °C for 48 h. The resulting gel was filtered, washed and calcined at 540 °C for 7 h. A white, porous material was obtained.

Chitosan-templated siliceous material synthesis

A solution of 0.2 ml acetic acid in 13.3 ml double-distilled water was prepared. Then, 6.2 g Na_2SiO_3 contained in 12.2 ml aqueous solution was added. After stirring for 10 min, a solution of 0.05 g chitosan in 16.75 ml 1% v/v acetic acid was added, followed by 30 min of stirring. Then, 6.6 ml water was added and the gel was stirred for 30 min. The mixture was autoclaved at 140 °C for 48 h. The resulting gel was filtered, washed and calcined at 540 °C for 7 h. A grey and white, porous, fragile monolithic material with a fibrous aspect was obtained (Fig. 2).
When chitosan solution was mixed with the silicate solution, a viscous, white gel was formed.

Characterisation

Mercury porosimetry experiments were run on a Carlo Erba porosimeter 2000.
Wide-angle X-ray diffractograms were made using a Phillips PW 1710 diffractometer with a copper anode and a curved graphite monochromator.
Transmission electron microscopy was performed with a Jeol 100 CX II transmission electron microscope operating at 100 kV with a magnification of 100 000×. Observations were made at bright field. Powdered samples were placed on copper supports of 2000 mesh.
Scanning electron microscopy runs were made with a Jeol 35 scanning electron microscope operating between 15 and 21 eV, with a Si–Li dispersive energy microanalysis system, 140-eV resolution and SYS-EDAX image analysis software.
The nitrogen adsorption isotherms at 77.6 K were measured with an Micrometrics Accusorb 2100 E instrument. Each sample was degassed at 373 K for 6 h at a pressure of 10^{-4} Pa.
Samples were observed using a Zeiss polarising microscope.

Results

The wide-angle X-ray diffractograms of both samples showed a broad band centred at about 4.4 Å of amorphous silica. No significant differences were seen between samples. No birefringence was detected by

Fig. 2 Photography of a monolith of chitosan-templated siliceous material (*CTSM*). Length about 4 cm

polarised light microscopy in any sample, confirming the presence of amorphous silica.

The mercury porosimetry results are shown in Figs. 3 and 4. They also show the $dV/d \log R$ versus pore radius curves, which are interpreted as the pore size distribution, R being the pore radius. The MCM-41 pore size distribution was fitted with a Poisson distribution with an average pore radius of 2.67 ± 0.19 μm and a standard deviation of 2.08 μm. The chitosan-templated siliceous material porosimetry data could be fitted with a Gaussian distribution whose parameters were an average pore radius of 0.57 ± 0.23 μm and a standard deviation of 0.19 μm. The adsorption–desorption isotherms and the mesopore size distributions are presented in Figs. 5 and 6. The isotherm of MCM-41 is of type IV, typical of mesoporous solids; however, the adsorption isotherm shape at $p/p_0 > 0.95$ suggested that the intercrystallite macropores were filled and that multilayer deposition occurred. The chitosan-templated sample shows a type II isotherm, which is obtained in macroporous adsorbents [50]. The inflection in the adsorption isotherm indicates the mesopore filling. The coordinate of the inflection point depends on the pore

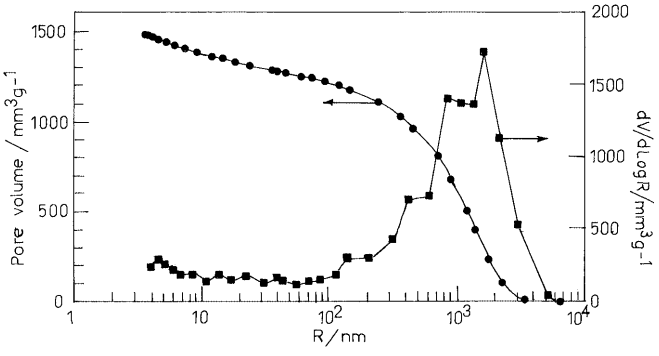

Fig. 3 Pore volume (●) versus pore radius obtained by mercury intrusion porosimetry and $dV/d \log R$ (■) versus pore radius of MCM-41

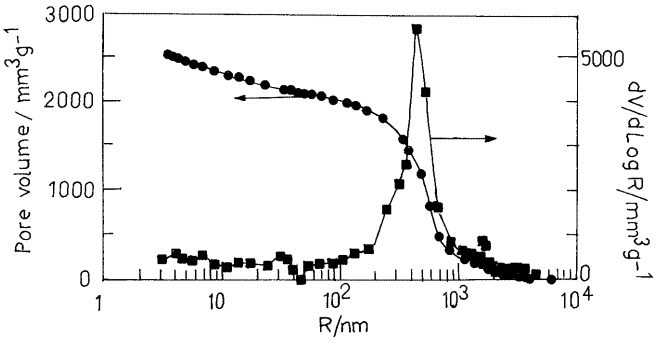

Fig. 4 Pore volume (●) versus pore radius obtained by mercury intrusion porosimetry and $dV/d \log R$ (■) versus pore radius of CTSM

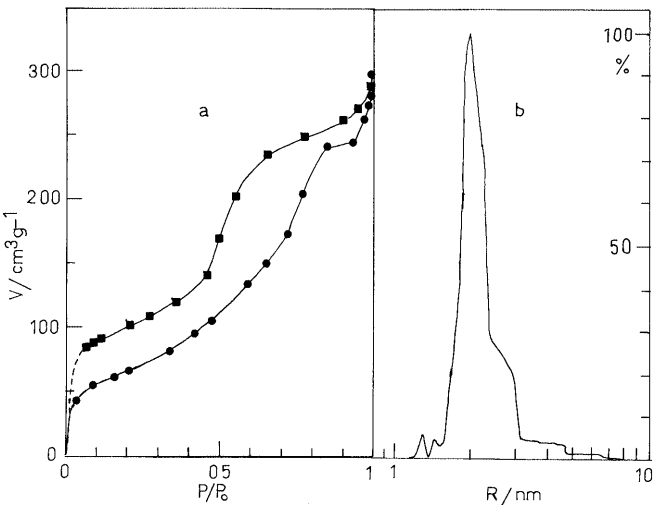

Fig. 5 **a** Adsorption (●) – desorption (■) of nitrogen on MCM-41. **b** dV/dR versus pore radius

size. Hysteresis loops of type H2 may be seen in the figures, which are associated with capillary condensation taking place in mesopores [50] with both ends open [51]. According to de Boer [52] this type of hysteresis loop appears when the capillaries are regular or irregular cylinders or prisms open at both ends. Furthermore, the desorption hysteresis at low p/p_0 values indicates micropore filling. According to Cohan [53] no pores of actual radii less than about a molecular diameter could be effective in causing hysteresis (actually, the critical radius was taken to be two molecular diameters), and Cohan showed that for a number of systems the desorption branch rejoined the adsorption one at p/p_0 values corresponding to pore radii close to twice the estimated size of the adsorbate molecules. The plot of the derivative of the pore volume per unit weight versus the pore radius (dV/dR) is shown in Figs. 5b and 6b. Some micropores (whose radius is about 1 nm) are present in both samples, as can be seen in the pore size distribution plots. The sharp pore size distribution of MCM-41 confirms that the mesopores are exceptionally uniform, with an average pore radius of 2.1 ± 0.4 nm; however, the chitosan-templated sample has a multimodal pore size distribution. It has sharp bands centred at pore radii of 0.84, 1.0, 1.2 and 1.5 nm and a broad band between 3 and 10 nm. The MCM-41 Brunguer–Emmett–Teller surface area was 360 ± 150 m^2 g^{-1} and that of the chitosan-templated siliceous material was 22.1 ± 1.7 m^2 g^{-1}.

The uniform mesopore structure of the MCM-41 sample was evidenced by the transmission electron microscope lattice image shown in Fig. 7. The image of the calcined sample shows the regular hexagonal array of uniform channels that is characteristic of MCM-41. When viewed perpendicular to the channels

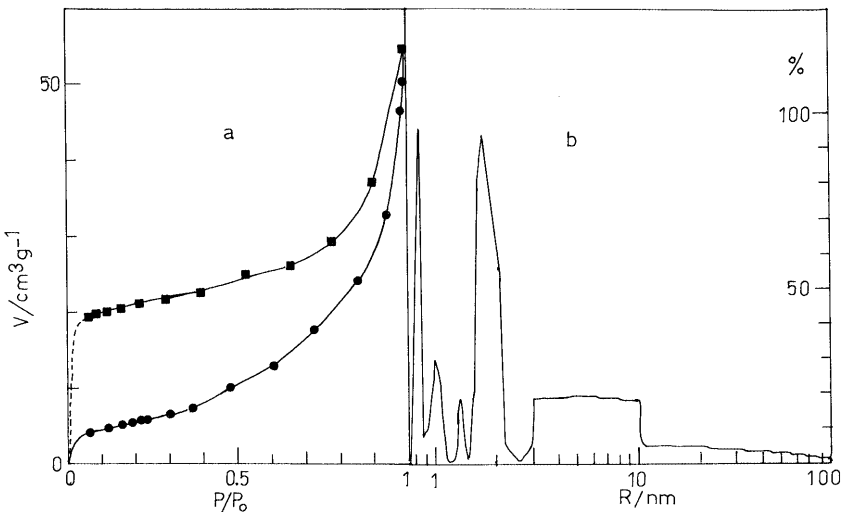

Fig. 6 **a** Adsorption (●) – desorption (■) of nitrogen on CTSM. **b** dV/dR versus pore radius

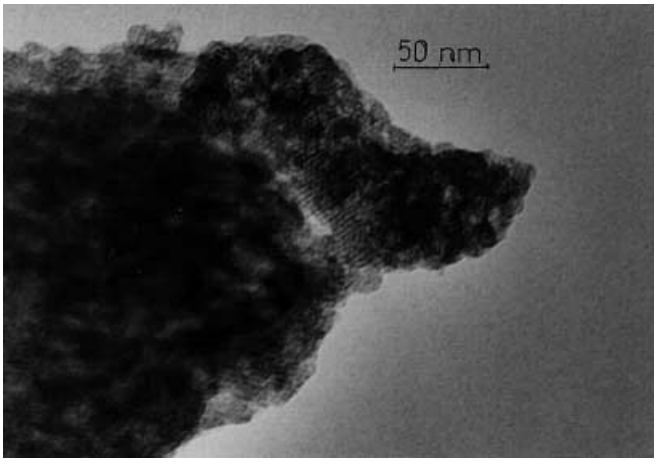

Fig. 7 Transmission electron micrograph of MCM-41, showing patches composed of regular rows viewed perpendicular to the mesopores axis

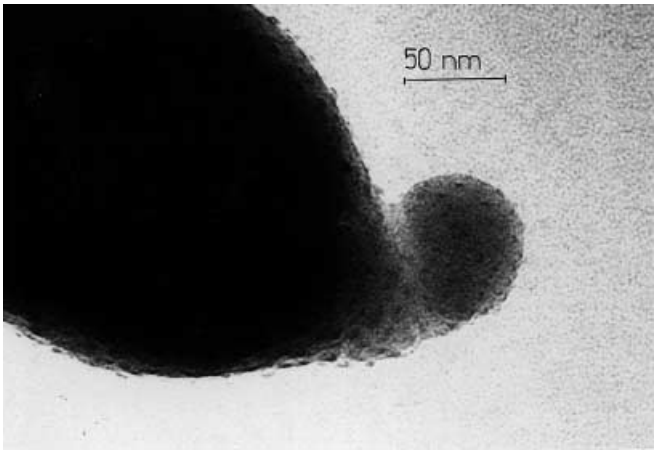

Fig. 8 Transmission electron micrograph of CTSM, showing a less-regular array of channels than that of MCM-41. The channels were in general, parallel

axis, the pores were seen to be arranged in patches composed of regular rows. The usual hexagonal structure with each pore surrounded by six neighbours was detected.

The chitosan-templated material shows a less-regular array of larger channels, which, in general, were parallel, as can be seen in the transmission electron microscope image shown in the Fig. 8. The macroscopic fibrous aspect shown by the monolith in Fig. 2 was retained at relatively low magnification, as can be seen in the electron scanning micrograph in Fig. 9. A 40-fold magnification (Figs. 10, 11) shows the macroporous structure, which seems to be bicontinuous.

Observations using a polarising microscope on calcined samples suspended in water show low birefringence (with no recognisable texture) in some regions of the MCM-41 sample and no birefringence in the sample of chitosan-templated siliceous material.

Discussion

MCM-41 prepared with CTAB as a template by hydrothermal synthesis typically has a pore radius of about 1.5–1.8 nm and a surface area of about 1000–1240 $m^2\ g^{-1}$ [54, 55]. MCM-41 prepared with the method described here has a similar pore radius (2.1 ± 0.4 nm) but smaller specific area (360 ± 150 $m^2\ g^{-1}$). The order in the mesopores is probably responsible for the slight birefringence of this material.

Sonwane et al. [55] pointed out that mesoporous MCM-41 materials comprise several levels of structure (mesopores, crystallites, grains and particles), each

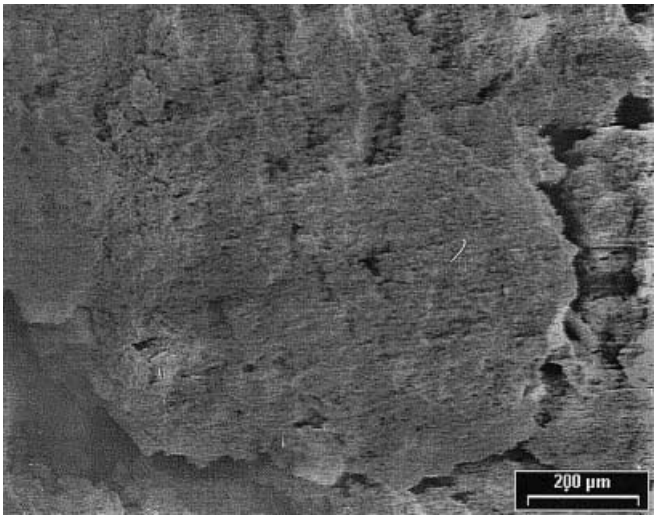

Fig. 9 Low-magnification scanning electron micrograph of CTSM, showing the general orientation of the structure

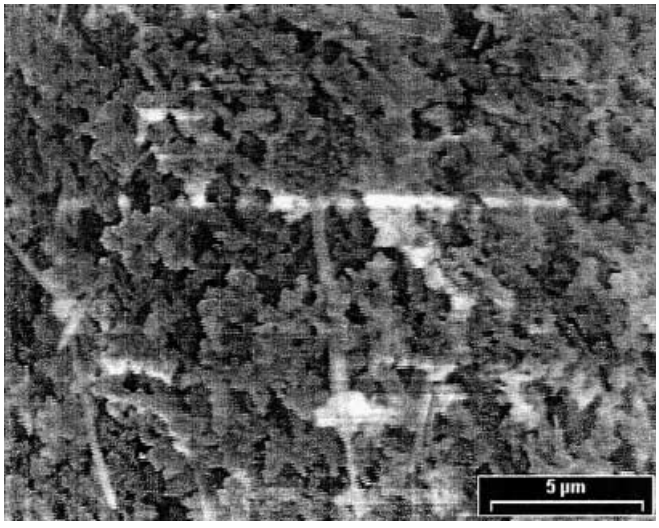

Fig. 11 High-magnification scanning electron micrograph of CTSM, showing a spongelike structure

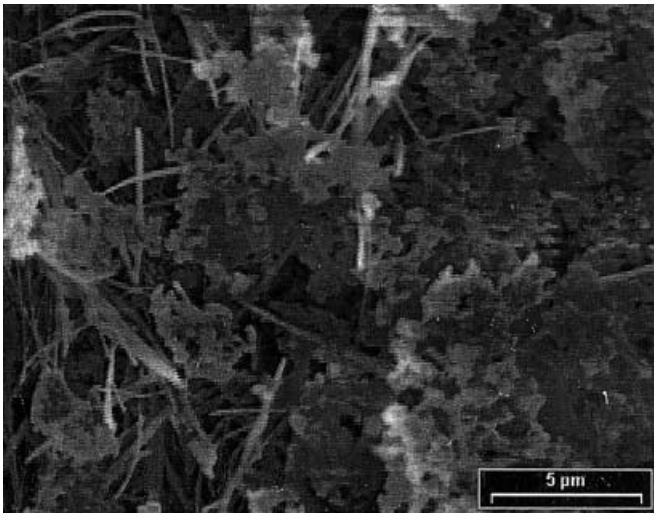

Fig. 10 High-magnification scanning electron micrograph of CTSM, showing a bicontinuous structure

having its characteristic length scale spanning over 4 decades of resolution. By mercury intrusion porosimetry, they found that MCM-41 materials have a macroporous fractal dimension of 2.7–3 and that the grain dimensions range from 0.1 to 0.4 μm. The fractal dimension of the mesopores was 2 and they are therefore very smooth. The walls of the mesopores may collapse at higher pressures of mercury, whereas at very low pressures, mercury intruded into the interparticle space. This corresponds to a macropore size of 0.35 μm or larger (pressure lower than 2 MPa). The crystallite size is about 8–25 nm. We found an average macropore radius of 2.67 $\pm$ 0.19 μm in the MCM-41 sample.

The sample of chitosan-templated siliceous material showed no birefringence in the polarising microscope, which indicates that the distribution of pores was not ordered.

The sample of chitosan-templated siliceous material had a multimodal pore size distribution, with radii ranging from 0.84 to 0.57 μm. This seemed to reflect the formation of chitosan fibrous aggregates. The pore size and the connectivity follow the structure of the template aggregates, i.e., the resulting silica gel network is a precise copy of the original self-assembly structure [56]. The smaller pore sizes were commensurable to the *a* and *b* crystallographic parameters of chitosan. This suggests that bundles of parallel hydrated chitosan helices were formed in solution, which is in accord with literature information about pure chitosan solutions. [29, 33, 40]. Those smaller bundles were arranged in a parallel distribution of aggregates, but the spatial organisation was not hexagonal as in MCM-41 materials, as can be seen in the higher magnification transmission electron microscope photographs (Fig. 8). The higher magnification pictures were similar to Fig. 1 of Ref. [56], indicating that fibres were arranged in a slightly disordered bidimensional cubic fashion. Some pores were photographed perpendicular to the axis, showing that they were tubular channels.

It seems that the addition of silicate promoted the formation of supramolecular aggregates as occurs for other polysaccharides on addition of electrolyte, [44]. The addition of silicate may have induced the formation of a gel, with cross-linking of multiple helices in a three-dimensional network. This may be the origin of the spongelike structure viewed by scanning electron microscopy at higher magnifications. The pore size of that

structure is about 0.5 μm and thus corresponds to the pore size determined by mercury intrusion porosimetry. On a larger size scale, the material was fibrous, which may mean that there was preferential orientation of the system as a whole parallel to the axis of the tube in which the sample was made. There are several examples of orientation of mesoporous materials by surfaces (such as mica, graphite, hydrocarbons or air) in contact with the gel during the synthesis [57–63].

Krämer et al. [56] used some cationic and anionic block copolymers with polyelectrolyte behaviour as structure-directing media in a sol–gel process to synthesise nanoporous silica and found that depending on the relative block lengths and the salt content in the reaction mixture, different aggregation structures were obtained, leading to silica compounds with different pore sizes and architectures.

In summary, a fibrous material was obtained, whose macroscopic fibres consisted of a spongelike siliceous network with pores having radii of 0.57 $\pm$ 0.23 μm. The siliceous walls of the pores were, in turn, formed out of a microporous–mesoporous material; the pore radius distribution was polymodal with maxima at 0.84, 1.0, 1.2 and 1.5 nm and a broad band between 3 and 10 nm.

Concluding remarks

- It was demonstrated that the synthesis of siliceous porous material can be performed using chitosan as a template in a hydrothermal way.
- A fibrous material was obtained, whose macroscopic fibres consisted of a spongelike siliceous network with pores having radii of 0.57 $\pm$ 0.23 μm. The siliceous walls of the pores were, in turn, formed out of a microporous–mesoporous material; the pore radius distribution was polymodal with maxima at 0.84, 1.0, 1.2 and 1.5 nm and a broad band between 3 and 10 nm.
- The structure may be due to the aggregation of the hydrated chitosan helices in bundles of parallel fibres with different size and the gelation of the system. The process might be induced by the addition of silicate.

Acknowledgements This work was supported by a grant from the Universidad Nacional del Sur. M.A.M. is an assistant researcher of the Consejo Nacional de Investigaciones Científicas y Técnicas de la República Argentina.

References

1. Mercier L, Pinnavaia TJ (1997) Adv Mater 9:500
2. Llewelyn PL, Ciesla U, Decher H, Stadler R, Schuth F, Unger KK (1994) Stud Surf Sci Catal 84:2013
3. Grun M, Kurganov AA, Schacht S, Schuth F, Unger KK (1996) J Chromatogr A 740:1
4. Beck JS, Vartuli JC, Roth WJ, Leonowicz ME, Kresge CT, Schmitt KD, Chu CTW, Olson DH, Sheppard EW, McCullen SB, Higgins JB, Schlenker JL (1992) J Am Chem Soc 114:10834
5. Kresge CT, Leonowicz ME, Roth WJ, Vartuli JC, Beck JS (1992) Nature 359:710
6. Zhao DY, Yang PD, Huo QS, Chmelka BF, Stucky GD (1998) Curr Opin Colloid Interface Sci 3:174
7. Zhao DY, Feng JL, Huo QS, Melosh N, Freddrickson GH, Chmelka BF, Stucky GD (1998) Science 279:548
8. Krämer E, Förster S, Götner C, Antonietti M (1998) Langmuir 14:2027
9. Davis SA, Burkett SL, Mendelson NH, Mann S (1997) Nature 385:420
10. Beginn U (1998) Adv Mater 10:1391
11. Shahidi F (1995) Can Chem News 47:25
12. Sashiwa H, Simoto H, Shigenmasa Y, Ogawa K, Tokura S (1991) Carbohydr Polym 16:291
13. Sashiwa H, Saimoto H, Shigenmasa Y, Tokura E (1991) In: Sanford CJ, Sizakis JP (eds) Advances in chitin and chitosan. Elsevier, London, p 145–156
14. Nyström B, Kjøniksen A-L, Iversen C (1999) Adv Colloid Interface Sci 79:81
15. Yui T, Imada K, Okayama K, Obata Y, Suzuki K, Ogawa K (1994) Macromolecules 27:7601
16. Cairas P, Miles MJ, Morris VJ, Ridout MJ, Brownsey GJ, Winter WT (1992) Carbohydr Res 235:23
17. Mazeau K, Winter WT, Chanzy H (1994) Macromolecules 27:7606
18. Ogawa K, Nakata K, Yamamoto A, Niita Y, Yui T (1996) Chem Mater 8:2349
19. Clark GL, Smith AF (1937) J Phys Chem 40:863
20. Ogawa K, Hirano S, Miyanishi T, Yui T, Watanabe T (1984) Macromolecules 17:973
21. Ogawa K, Oka K, Miyanishi T, Hirano S (1984) In: Zakiris JP (ed) Chitin, chitosan and related enzymes. Academic, Orlando, pp 327–435
22. Park JW, Choi K-H (1983) Bull Korean Chem Soc 4:68
23. Rinaudo M, Domard A (1989) In: Skjåk-Braek G, Anthonsen T, Sanford P (eds) Chitin and chitosan. Elsevier, London, pp 71–86
24. Jocic D, Juliá MR, Erra P (1996) Colloid Polym Sci 274:357
25. Amiji MM (1995) Carbohydr Polym 26:211
26. Vårum KM, Ottøy MH, Smidarød O (1994) Carbohydr Polym 25:65
27. Anthonsen MW, Vårum KM, Smidarød O (1993) Carbohydr Polym Sci 22:193
28. Chen R-H, Lin W-C (1992) J Fish Soc Taiwan 19:299
29. Wu C, Zou S, Wang W (1995) Biopolymers 35:385
30. Berth G, Dautzenberg H, Peter MG (1988) In: Domard A, Roberts GAF, Vårum KM (eds) Advances in chitin science. Proceedings of the 7th International Conference on Chitin, Chitosan and Euchis'97. Andre, Jacques André Publisher Lyon (France) pp 429–436
31. Smisrød, O, Ottøy MH, Anthonsen MW, Vårum KM (1988) In: Domard A, Roberts GAF, Vårum KM (eds) Advances in chitin science. Proceedings of the 7th International Conference on Chitin, Chitosan and Euchis'97. Andre, pp 402–409
32. (a) Moore GK, Roberts GAF (1979) Int J Biol Macromol 2:73; (b) Moore GK, Roberts GAF (1979) Int J Biol Macromol 2:78
33. Delben F, Lapsin R, Pircl S (1990) Int J Biol Macromol 12:9

34. Yamoto H, Amaike M, Saito H (1995) Biometics 3:123
35. Draget KI (1996) Polym Gel Networks 4:143
36. Brack HP, Tirmizi SA, Risen WM (1997) Polymer 38:2351
37. Kjøniksen A-L, Nyström B, Nakken T, Palmgren O, Tande T(1997) Polym Bull 38:71
38. Bianchi E, Marsano E, Tacchino A (1997) Carbohydr Polym 32:23
39. Domard A, Cartier N (1992) Int J Biol Macromol 14:100
40. Iversen C, Kjøniksen A-L, Nyström B, Nakken T, Palmgren O, Tande T (1997) Polym Bull 39:747
41. Yamaguchi R, Hirano S, Arai I, Ito T (1978) Agric Chem 42:1981
42. Domard A (1998) In: Domard A, Roberts GAF, Vårum KM (eds) Advances in chitin science. Proceedings of the 7th International Conference on Chitin, Chitosan and Euchis'97. Andre, pp 410–420
43. Ratto J, Hatakeyama T, Blumstein RB (1995) Polymer 15:2915
44. Clark A (1996) Curr Opin Colloid Interface Sci 1:712
45. Berth G, Dautzenberg H, Christensen BE, Harding SE, Rother G, Smidsrod O (1996) Macromolecules 29:3491
46. Miles M, Rinaudo M, Duplessix R, Borsali R, Lindner P (1995) Macromolecules 28:3119
47. Miles M, Lindner P, Rinaudo M, Borsali R (1996) Macromolecules 29:473
48. Viebke C, Borgstrom J, Piculell L (1995) Carbohydr Polym 27:145
49. Turquois T, Rochas C, Taravel F-R, Doublier JL, Axelos MAV (1995) Biopolymers 35:227
50. Sing KSW, Everett DH, Haul RAW, Moscou L, Pierotti RA, Rouquérol J, Siemieniewska T (1985) Pure Appl Chem 57:603
51. Cohan LH (1938) J Am Chem Soc 60:433
52. de Boer JH (1958) The structure and properties of porous materials. Butterworths, London, p 68
53. Cohan LH (1944) J Am Chem Soc 66:98
54. Namba S, Mochizuki A, Kito M (1998) In: Bonneviot L, Béland F, Danumah C, Giasson S, Kaliaguine S (Eds) Mesoporous molecular sieves. Elsevier, Amsterdam, p 257–264
55. Sonwane CG, Bhatia SK, Calos NJ (1999) Langmuir 15:4603
56. Krämer S, Förster S, Göltner C, Antonietti M (1998) Langmuir 14:2027
57. Yang H, Kuperman A, Coombs N, Mamicheafara S, Ozin GA (1996) Nature 379:703
58. Yang H, Coombs N, Sokolov I, Ozin GA (1996) Nature 381:589
59. Yang H, Coombs N, Sokolov I, Ozin GA (1997) J Mater Chem 7:1285
60. Aksay JA, Trau M, Manne S, Honma I, Yao N, Zhou L, Fenter P, Eisenberger PM, Gruner SM (1996) Science 273:892
61. Manne S, Cleveland JP, Gaub HE, Stucky GD, Hansma PK (1994) Langmuir 10:4409
62. Manne S, Schaffer TE, Huo Q, Hansma PK, Morse DE, Stucky GD, Aksay IA (1997) Langmuir 13:6382
63. Tolbert SH, Schaffer TE, Feng JL, Hansma PK, Stucky GD (1997) Chem Mater 9:1962